Journal of Alloys and Compounds 509 (2011) 4098–4103

Contents lists available at ScienceDirect

Journal of Alloys and Compounds

journal homepage: www.elsevier.com/locate/jallcom

# Synthesis of lanthanum hydroxide and lanthanum oxide nanoparticles by sonochemical method

Masoud Salavati-Niasari[a,b,*], Ghader Hosseinzadeh[a], Fatemeh Davar[a]

[a] Institute of Nano Science and Nano Technology, University of Kashan, P. O. Box. 87317–51167, Kashan, Islamic Republic of Iran
[b] Department of Inorganic Chemistry, Faculty of Chemistry, University of Kashan, P. O. Box. 87317–51167, Kashan, Islamic Republic of Iran

ARTICLE INFO

*Article history:*
Received 23 June 2010
Accepted 12 July 2010
Available online 16 July 2010

*Keywords:*
$La(OH)_3$
Sonochemical
Nanoparticles
$La_2O_3$

ABSTRACT

In this work lanthanum hydroxide nanoparticles were synthesized by sonochemical method. $La_2O_3$ nanoparticles were obtained after calcination of the $La(OH)_3$ nanoparticles precursor in air at 600 °C for 2 h. The effect of some parameters such as concentration of precursors, pulse time of sonication, time of sonication, and addition of PEG as surfactant on the morphology and the particle size were studied. The as-prepared products were characterized by X-ray diffraction (XRD), scanning electron microscopy (SEM), transmission electron microscopy (TEM), X-ray photoelectron spectrum (XPS) and Fourier transform infrared (FT-IR) spectra.



## 1. Introduction

The synthesis, production and manipulation of materials on the nanoscale is currently one of the favorable areas of research which also attracts the industrialists for designing and fabricating new functional materials with novel special properties [1,2]. Because of their unique electronic configuration [4f electrons] lanthanides have been applied in various fields; also these lanthanide-based materials have attractive and interesting magnetic [3], optical [4,5], electrical and therapeutic [6] properties. Among the lanthanides, lanthanum has been extensively examined for its unique properties [7–12]. And lanthanum have been synthesized in various compositions such as $La(OH)_3$ [13], $LaF_3$ [5], $La_2(CO_3)_3$ [14], $LaPO_4$ [15–17], $LaBO_3$ [18], LaOF [19], $La_2Sn_2O_7$ [20], $La_2O_3$ [21] nanoparticles.

Although many methods have been developed for the synthesis of lanthanum nanostructures including hydrothermal [22], solvothermal [23], micro emulsion or reverse micelles [24], sol–gel [25], laser deposition [26] and other chemical and physical methods; but some of these methods are affected from long reaction time, high temperature, high pressure, expensive surface materials)surfactant) and so on.

In 1999 a simple, effective and novel route, i.e. sonochemical method, developed to prepare nanostructures [27]. Recently, ZnO nanorod/Ag nanoparticle composites have been successfully prepared by Li et al. via sonochemical process [28]. A sonochemical method has been used for synthesized $MnO_2$ nanoparticles inside the pore channels of carbon by Zhu et al. [29]. Nanosized copper aluminate particles were synthesized using a precursor method with the aid of ultrasound irradiation [30].

In this work lanthanum hydroxide nanoparticles were successfully prepared from the reaction of lanthanum acetate and NaOH by sonochemical method. Then, lanthanum oxide nanoparticles were prepared from the calcinations of resulted product at 600 °C. Also, effects of weight ratio or molar ratio of $NaOH/La(OAC)_3$ on size and morphology of products were examined. As-prepared products were characterized by powder X-ray diffraction (XRD), scanning electron microscopy (SEM) transmission electron microscopy (TEM), X-ray photoelectron spectrum (XPS) and FT-IR spectroscopy.

## 2. Experimental

### 2.1. Materials and physical measurements

All the chemicals reagents used in our experiments were of analytical grade and were used as received without further purification. A multiwave ultrasonic generator (Sonicator 3000; Bandeline, MS 72, Germany), equipped with a converter/transducer and titanium oscillator (horn), 12.5 mm in diameter, operating at 20 kHz with a maximum power output of 60 W, was used for the ultrasonic irradiation. The ultrasonic generator automatically adjusted the power level. The wave amplitude in each experiment was adjusted as needed. XRD patterns were recorded by a Rigaku D-max C III, X-ray diffractometer using Ni-filtered Cu Kα radiation. Elemental analyses were obtained from Carlo ERBA Model EA 1108 analyzer. X-Ray Photoelectron Spectroscopy (XPS) of the as-prepared products were measured on an ESCA-3000 electron spectrometer with nonmonochromatized Mg Kα X-ray as the excitation source. Scanning electron microscopy (SEM) images were obtained on Philips XL-30ESEM equipped with an energy dispersive X-ray spectroscopy. Transmission electron microscopy (TEM) images were obtained on a Philips EM208

* Corresponding author at: Institute of Nano Science and Nano Technology, University of Kashan, P. O. Box. 87317–51167, Kashan, Islamic Republic of Iran.
Tel.: +98 361 5555 333; fax: +98 361 555 29 30.
*E-mail address:* salavati@kashanu.ac.ir (M. Salavati-Niasari).

0925-8388/$ – see front matter © 2010 Elsevier B.V. All rights reserved.
doi:10.1016/j.jallcom.2010.07.083

**Table 1**
Experimental condition for the preparation of $La(OH)_3$ and $La_2O_3$.

| Sample no. | Pulsation | Calcinations' time at 600 °C (h) | Amount of NaOH (mmol) | Amount of $La(OAC)_3$ (mmol) | Weight ratio of NaOH/$La(OAC)_3$ | Molar ratio of NaOH/$La(OAC)_3$ | Time of sonication (min) | Amount of PEG (ml) |
|---|---|---|---|---|---|---|---|---|
| 1 | Off | – | 7.5 | 0.63 | 1.5 | 12 | 30 | – |
| 2 | Off | – | 7.5 | 0.95 | 1 | 8 | 30 | – |
| 3 | Off | – | 7.5 | 1.3 | 0.75 | 6 | 30 | – |
| 4 | Off | – | 5.0 | 2.6 | 0.25 | 2 | 30 | – |
| 5 | Off | – | 5.0 | 2.6 | 0.25 | 2 | 30 | 3 |
| 6 | Off | 2 | 5.0 | 2.6 | 0.25 | 2 | 30 | 3 |
| 7 | Off | 2 | 7.5 | 1.3 | 0.75 | 6 | 30 | – |
| 8 | 2 s on1 s off | – | 7.5 | 1.3 | 0.75 | 6 | 30 | – |
| 9 | 4 s on1 s off | – | 7.5 | 1.3 | 0.75 | 6 | 30 | – |
| 10 | 8 s on1 s off | – | 7.5 | 1.3 | 0.75 | 6 | 30 | – |
| 11 | Off | – | 7.5 | 1.3 | 0.75 | 6 | – | – |
| 12 | Off | – | 0.5 | 2.6 | 0.25 | 2 | 15 | – |
| 13 | Off | – | 0.5 | 2.6 | 0.25 | 2 | 45 | – |

transmission electron microscope with an accelerating voltage of 100 kV. Fourier transform infrared (FT-IR) spectra were recorded on Shimadzu Varian 4300 spectrophotometer in KBr pellets.

### 2.2. Preparation procedure

Different amounts of dissolved NaOH in 30 ml water were added dropwise to the solution of lanthanum acetate with different concentration and were sonicated for 15, 30 and 45 min with high-density ultrasonic probe immersed directly into the solution according to Table 1. The resulted products were collected by centrifugation 6000 rpm and were washed three times with distilled water and dried at 50 °C in oven (Scheme 1). In order to investigate the effect of pulsation on the morphology and size of obtained nanoparticles, pulses were carried out with different periodic time to the solutions (Table 1). To investigate the role of surfactant 3 ml of polyethylene glycol 600, (PEG), were added to the lanthanum acetate solution and then the resulted product was washed with distilled water several times for removing all of the PEG and then, pure sample was obtained.

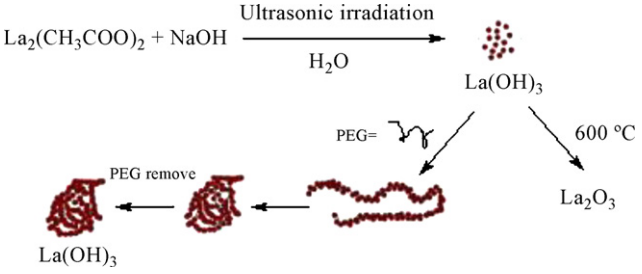


**Scheme 1.** Materials produced and formation methods of $La_2O_3$.

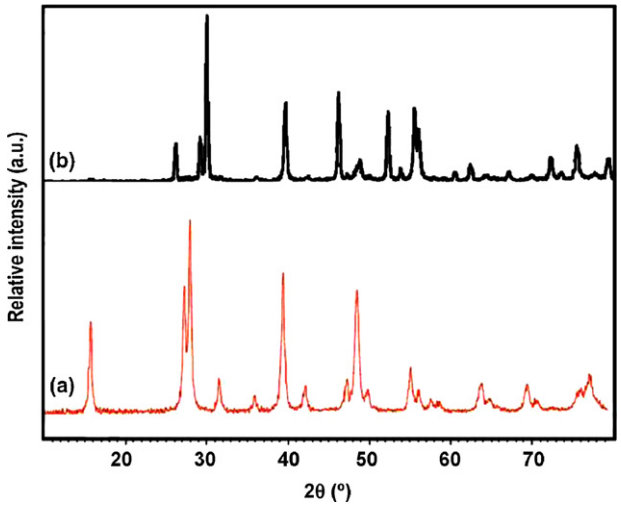


**Fig. 1.** XRD patterns of (a) sample no. 10 and (b) sample no. 7.

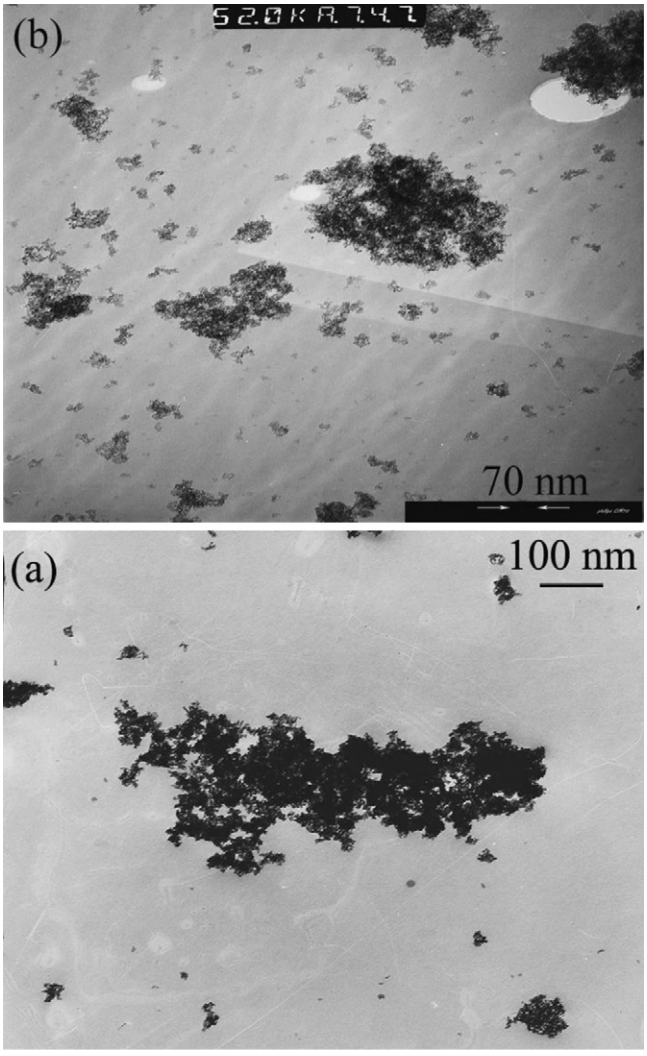


**Fig. 2.** TEM images of (a) sample no. 10 and (b) sample no. 7.

## 3. Results and discussion

Shown in Fig. 1a is the wide-angle XRD pattern of sample no. 10. All of the diffraction peaks can be indexed to the hexagonal structure of $La(OH)_3$ (space group *P*-3*m*1) which is very close to the values in the literature (JCPDS No. 36-1481 with cell constant $a = 6.5286$ Å, $b = 6.5286$ Å and $c = 3.8588$ Å). The broadening of the peaks indicated that the particles were of nanometer scale. The

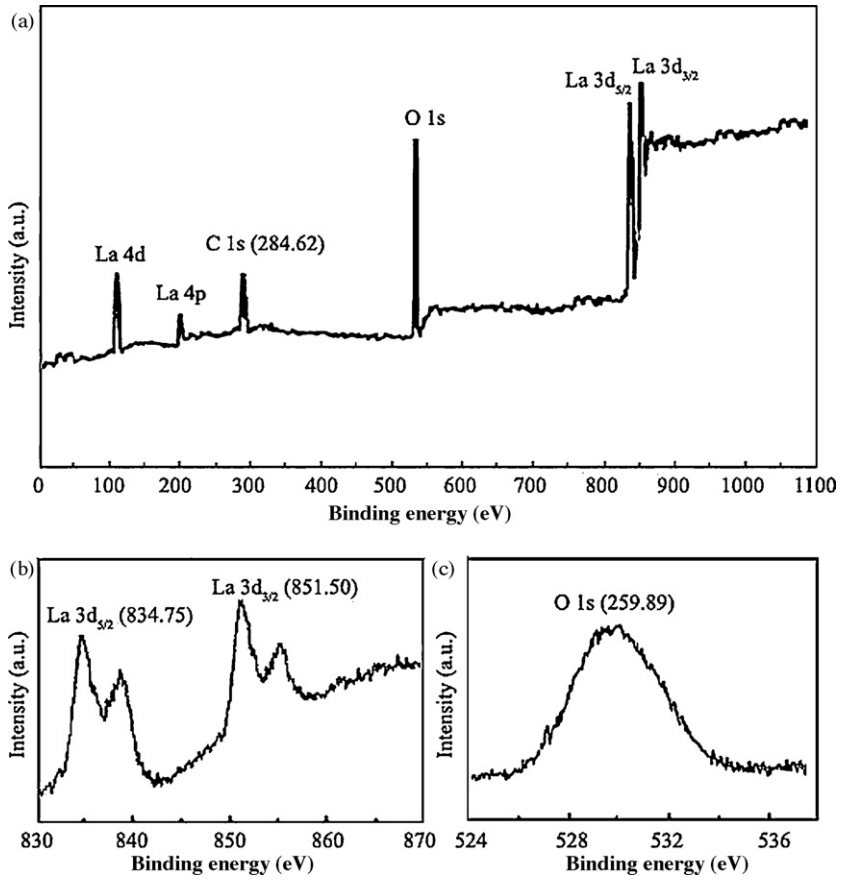


**Fig. 3.** XPS spectra of the $La_2O_3$, (sample no. 7): (a) survey spectrum, (b) La 3d region and (c) O 1s region.

average particle size of the obtained products was estimated from Debeys–Scherrer equation:

$$D_c = \frac{K\lambda}{\beta \cos\theta}$$

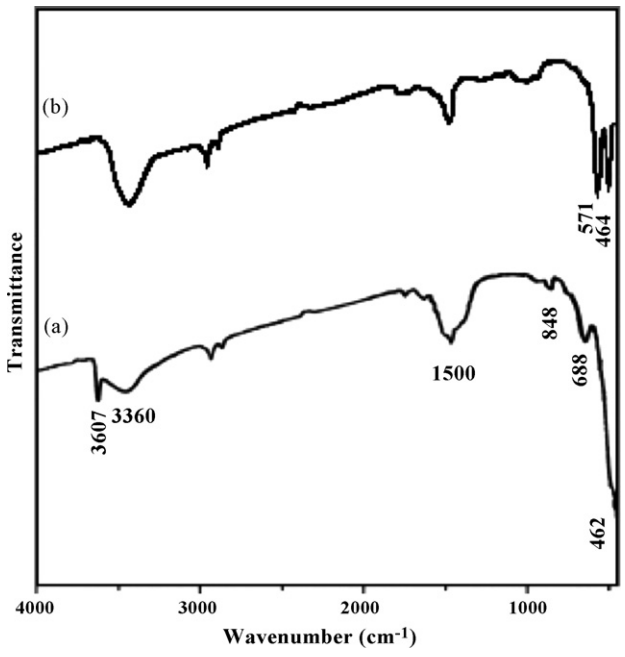


**Fig. 4.** FT-IR spectra of the as-synthesized products: (a) sample no. 10 and (b) sample no. 7.

where $\beta$ is the breadth of the observed diffraction line at its half-intensity maximum, $K$ is the so-called shape factor, which usually takes a value of about 0.9, and $\lambda$ is the wavelength of X-ray source used in XRD [31], was about 12 nm.

Fig. 1b shows the XRD pattern lanthanum oxide, sample no. 7, resulted from calcination of sample no. 10 at 600 °C for 2 h, from which we concluded that the $La_2O_3$ with high purity obtained and the pattern matches with $La_2O_3$ with hexagonal structure (space group *P*-3*m*1 with cell constant $a = 3.9381$ Å, $b = 3.9381$ Å and $c = 6.1361$ Å, JCPDS No.83-1344), the sharp diffraction peak the sample indicated that well crystallized lanthanum oxide crystals can be prepared under current synthetic procedure. The broadening of the peaks indicated that the particles were of nanometer scale. Average size of the particles was estimated from Scherrer equation, average particles size of the particles was 45 nm.

TEM photographs of the products have been given in Fig. 2. Fig. 2a and b show TEM images of $La(OH)_3$, sample no. 10, and $La_2O_3$, sample no.7, respectively. The size of nanoparticles obtained from the XRD diffraction patterns are in close agreement with the TEM studies which show sizes of $15 \pm 2$ nm for sample no.10, also the particles are observed to be agglomerated (Fig. 2a). Fig. 2b shows TEM image of $La_2O_3$ nanoparticles, sample no. 7, which also shows the average particle size of $La_2O_3$ is about $40 \pm 2$ nm.

Further evidence for the composition was illuminated by the XPS of the $La_2O_3$ (sample no. 7). The binding energies obtained in the XPS analysis were corrected for specimen by referencing the C 1s to 284.62 eV. The survey XPS spectrum of the product (Fig. 3a) suggests that there are no other metal elements on the surface of the sample except for La. Fig. 3b which shows that the binding energy of La $3d_{5/2}$ and La $3d_{3/2}$ are 834.75 and 851.50 eV, respectively [32,33]. In Fig. 3c, it can be seen that the O 1s profile is asymmetric, indi-

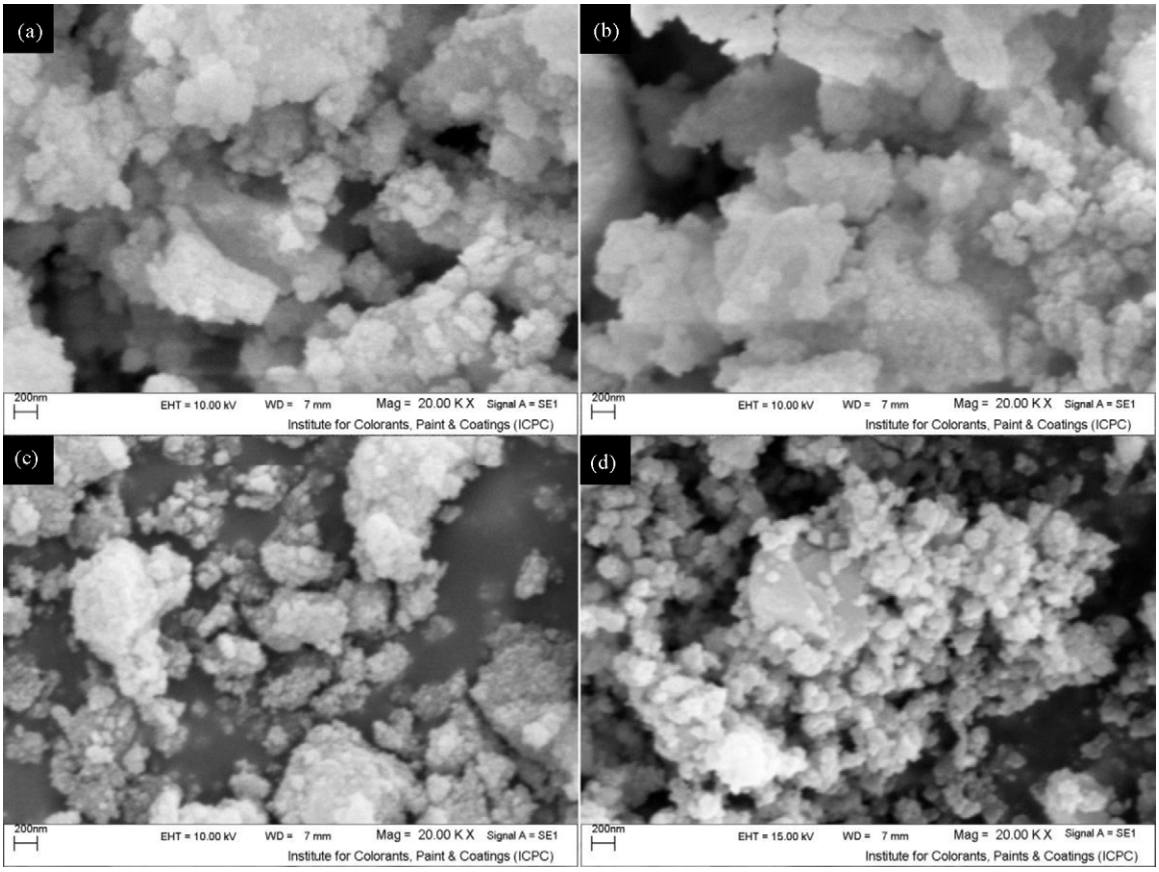


**Fig. 5.** SEM images of $La(OH)_3$ nanoparticles (a) sample no. 1, (b) sample no. 2, (c) sample no. 3, and (d) sample no. 4.

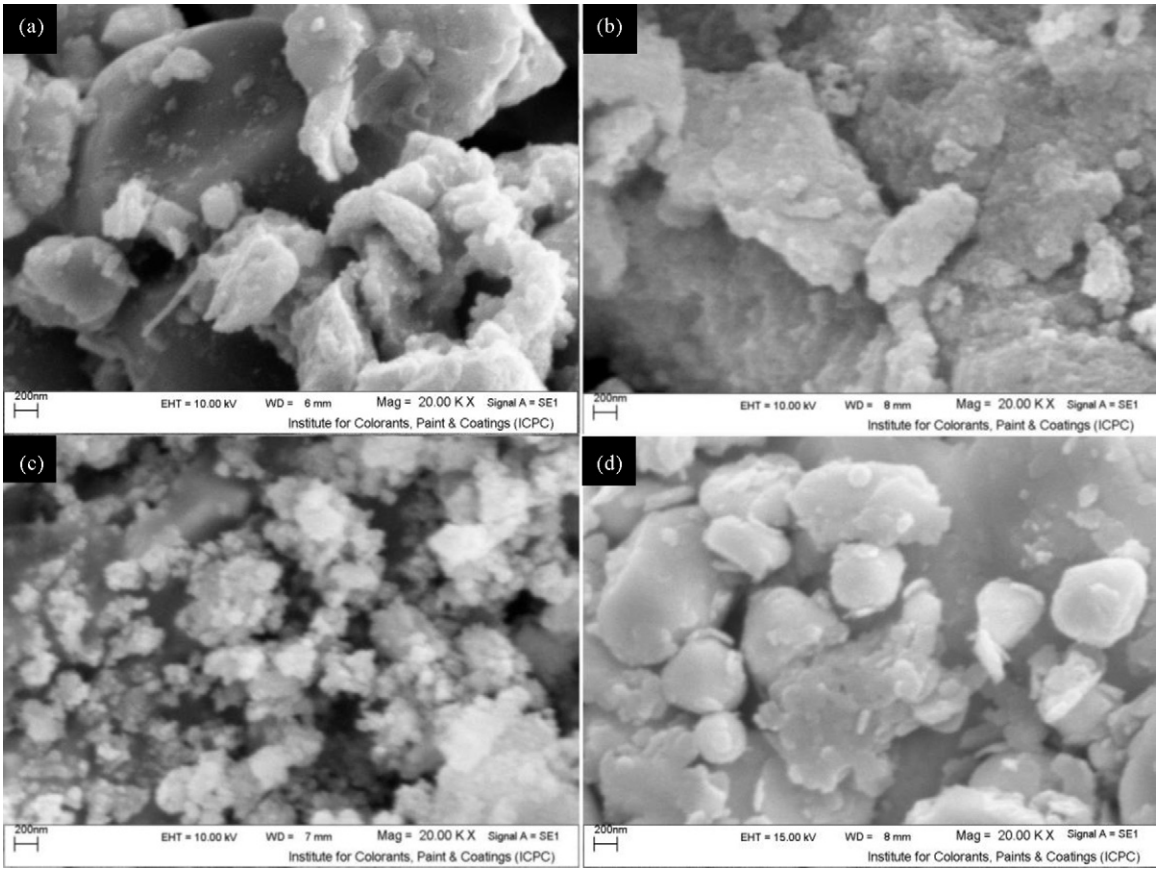


**Fig. 6.** SEM images of (a) sample no. 8, (b) sample no. 9, (c) sample no. 10 and (d) sample no. 11.

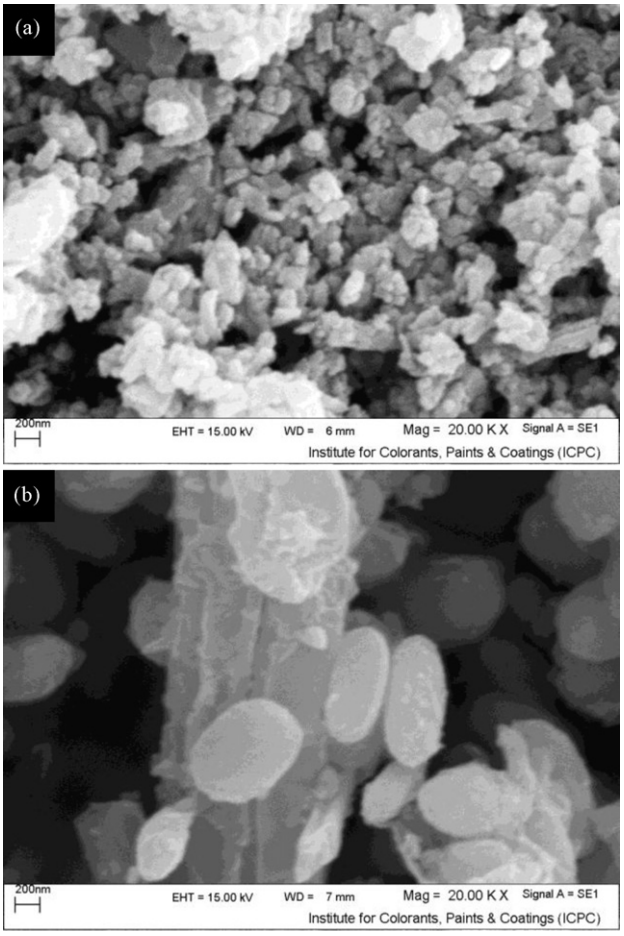


**Fig. 7.** SEM images of the $La(OH)_3$ nanoparticles: (a) sample no. 12 and (d) sample no. 13.

cating that two oxygen species are present in the nearby region. The peak which is about 529.89 eV can be indexed to the $O^{2-}$ in the $La_2O_3$

FT-IR spectra were recorded to show the functional groups for every product at each step of the synthesis. The infrared spectra of sample no. 10, and sample no. 7 are shown in Fig. 4. In IR spectrum of sample no. 10 we see that lanthanum hydroxide was synthesized but we see carbonate anion absorption (Isolated, planar $CO_3^{2-}$ anion has a $D_3h$ symmetry (Fig. 4a)). The absorption peak at 3360 $cm^{-1}$ in Fig. 4a is attributed to the stretching vibration of the O–H bond and the bending vibration of H–O–H from water molecules on the external surface of the samples during handling to record the spectra. According to Fig. 4b a sharp peak at 3607 $cm^{-1}$ is appeared which is assigned for stretching mode of $OH^-$ in $La(OH)_3$ (sample no. 10). The weak broad absorption bands at 1500–1435 $cm^{-1}$ are attributed to asymmetric stretching mode of $CO_3^{2-}$ group. The absorption bands at 848 and 688 $cm^{-1}$ can be assigned to the bending out of plane vibrations and in plane vibrations [34], respectively. These absorption bonds were related to the absorbed water and $CO_2$ on the surface of lanthanum hydroxide. A sharp peak was observed at about 462 $cm^{-1}$ which can be attributed to stretching vibration of the La–O bond. Fig. 4b shows IR spectrum of sample no 7 from which we can conclude that lanthanum oxide was synthesized from the calcinations of lanthanum hydroxide at 600 °C for 2 h. The carbonate and water absorption bonds can be seen at this temperature because of basic character of lanthanids that absorb atmosphere water and carbon dioxide. In fact after absorption of water absorbed $CO_2$ form carbonate anion. It has been reported that $La_2O_3$ and $La(OH)_3$ are very sensitive to atmospheric conditions. When they are exposed to atmospheric carbon dioxide under ordinary conditions of temperature and pressure, the process of carbonation occurs, leading to the formation of surface carbonates or hydroxyl carbonates. For this reason storing of these compounds away from atmospheric condition is necessary [35–38]. In Fig. 4b the absorption band of carbonate ions were reduced and the absorption band of cubic phase $La_2O_3$ appears at 571 and 464 $cm^{-1}$.

In addition, some other conditions were examined to investigate the morphology changes of products, if any, and compare them with each other. One of key parameters which can be effective on particle size is molar ratio $NaOH/La(OAC)_3$. Fig. 5 shows SEM images of the lanthanum hydroxide nanoparticles prepared at different molar ratio for $NaOH/La(OAC)_3$ sonicated for 30 min. In sample no. 1 (sonication at highest ratio of $NaOH/La(OAC)_3$) we see smallest particles that have stuck together because the concentration of lanthanum acetate in solution is low and therefore causes concentration of resulted lanthanum hydroxide to be low on the other hand sonication power is primarily consumed for fragmentation and remained excess energy causes particles collide and stick together (Fig. 5a). In sample no. 2, (Fig. 5b), (sonication at low ratio of $NaOH/La(OAC)_3$ in comparison with sample no. 1) increasing amount of lanthanum acetate causes increasing concentration of resulted lanthanum hydroxide and consequently more consumption ultrasonic power for fragmentation lower excess energy for collision and lower stuck of particles in comparison with sample no. 1. We see this trend in sample no. 3 at which we increase the amount of lanthanum acetate and as a consequence the separation of particles increases (pay attention that in the samples 1 to 3 molar amount of NaOH is excess need for formation of $La(OH)_3$ and amount of lanthanum acetate limits amount of $La(OH)_3$), (Fig. 5c). In sample no. 4 the amount and concentration of $La(OH)_3$ is equal to sample no 2 but in sample no. 2 we have excess amount of NaOH and therefore pH is high so increasing pH value causes the particles stuck together (Fig. 5d).

In order to investigate the effects of pulsation on the size of obtained nanoparticles, pulsing was carried out on the solution with different periodic times (Fig. 6). In SEM image of sample no. 8 (2 s on 1 s off) it can be observed that the product mostly is aggregated (Fig. 6a). In SEM image of sample no. 9, (Fig. 6b), (4 s on 1 s off) fine particles are formed but stuck one another and sonication can not separate them, in fact sonication time was adequate only for forming tiny particles, not for separating particles from each other. Fig. 6c shows sample no. 10 (8 s on 1 s off) which tiny and separated particles were formed. Taking a look at Table 1, makes it clear that sample no. 3 (sonication at continuous state) and no. 10 (8 s on 1 s off) (Table 1) have the same conditions except pulsation. Figs. 5c and 6c show that both samples contain small particles; however, pulsation results in more separated particles. Fig. 6d shows the SEM image of sample no. 11 which was synthesized without ultrasonic treatment as a reference experiment. This image can help us to see the advantage of using ultrasonic treatment in the synthesis of $La(OH)_3$ nanoparticles. As can be observed, the successful preparation of nanosized products is indeed due to the ultrasonic treatment.

For investigating the effect of sonication time on the morphology of the lanthanum hydroxide, the reaction carried out in 15 and 45 min as well as. As Fig. 7a shows with decreasing aging time to 15 min (sample no. 12), the obtained particles were bigger than the particles of sample no. 4 with the aging time of 30 min. With increasing of the aging time to 45 min (sample no. 13) the nanoparticles with average size of 100 nm in diameter is produced, Fig. 7b.

Fig. 8 shows the surfactant effect on the morphology and size of nanoparticles of lanthanum hydroxide. In Fig. 8a (sample no. 5) we can see that added PEG keep particles Close together and spherical particles were formed (see Fig. 5d and compare with Fig. 8a). But

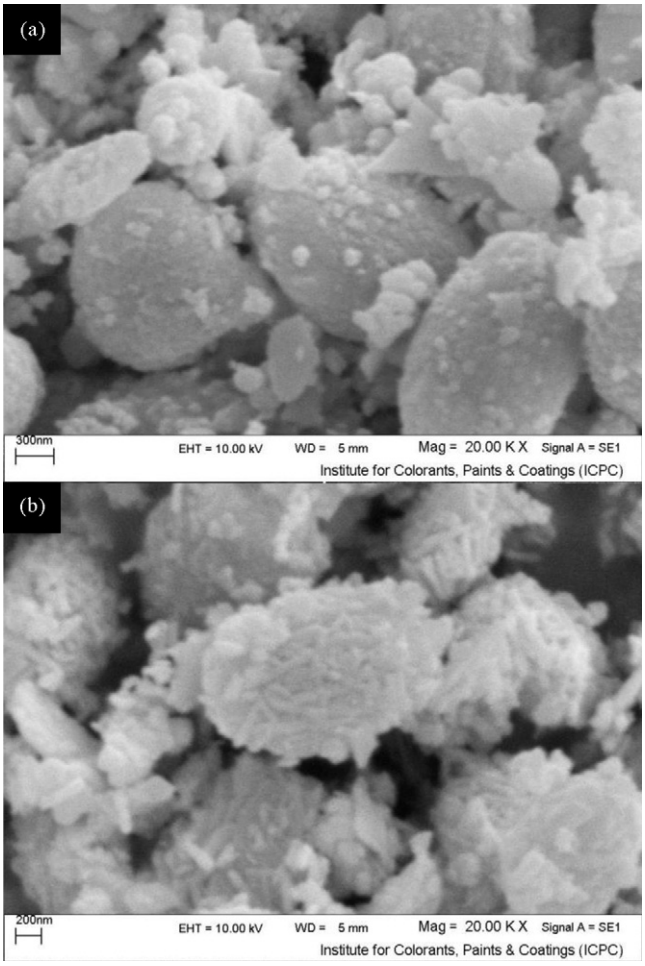


**Fig. 8.** SEM images of the $La(OH)_3$ nanoparticles: (a) sample no. 5, and (b) sample no. 6.

in Fig. 8b (sample no. 6) we see that spindle shape particles were formed in fact at Fig. 8a as well as spindle were formed, we concluded that in the presence of PEG formed nanoparticles absorb on the surface of PEG and nanowires were formed (presence of PEG cause formation of nanowires) this nanowires are winding and form spindle [25].

## 4. Conclusion

In summary, $La(OH)_3$ nanoparticles with the hexagonal structure type were synthesized by a sonochemical method. This method brings forward a broad idea to synthesize other rare-earth compounds with various morphologies and novel properties. Also, we have found a simple route to prepare $La_2O_3$ nanoparticles by facile thermal treatment of $La(OH)_3$. The XRD, TEM, SEM, XPS, and FT-IR were used to characterize the products. The effect of some parameters such as time of sonication, time period of pulse sonication, weight ratio or molar ratio of $NaOH/La(OAC)_3$, and addition of PEG as surfactant on the size and morphology of the obtained products were also investigated.

## Acknowledgements

Authors are grateful to the council of University of Kashan for their unending effort to provide financial support to undertake this work.

## References

[1] X.S. Fang, L. Zhang, J. Mater. Sci. Technol. 22 (2006) 1–18.
[2] X.S. Fang, C.H. Ye, L.D. Zhang, Y.H. Wang, Y.C. Wu, Adv. Funct. Mater. 15 (2005) 63–68.
[3] N. Wang, Q. Zhang, W. Chen, J. Cryst. Res. Technol. 42 (2007) 138–142.
[4] H.X. Mai, Y.W. Zhang, R. Si, Z.G. Yan, L.D. Sun, L.P. You, C.H. Yan, J. Am. Chem. Soc. 128 (2006) 6426–6436.
[5] X. Wang, J. Zhuang, Q. Peng, Y.D. Li, Inorg. Chem. 45 (2006) 6661–6665.
[6] S.P. Fricker, Chem. Soc. Rev. 35 (2006) 524–533.
[7] B. Lai, A.C. Johnson, H. Xiong, S. Ramanathan, J. Power Sources 186 (2009) 115–122.
[8] Y.C. Liu, Y.W. Chen, Ind. Eng. Chem. Res. 45 (2006) 2973–2980.
[9] C.L. Kuo, C.L. Wang, T.Y. Chena, G.J. Chen, I.M. Hung, C.J. Shih, K.Z. Fung, J. Alloys Compd. 440 (2007) 367–374.
[10] H. Wei, Y. Wu, N. Lun, F. Zhao, J. Mater. Sci. 39 (2004) 1305–1308.
[11] K. Rajesh, K.V. Baiju, M. Jayasankar, K.G. Warrierw, J. Am. Ceram. Soc. 91 (2008) 2415–2418.
[12] J. Sun, X.P. Qiu, W.T. Zhu, Int. J. Hydrogen Energy 30 (2005) 437–445.
[13] X. Wang, Y.D. Li, Angew. Chem. Int. Ed. 41 (2002) 4790–4793.
[14] P. Jeevanandam, Y. Koltypin, O. Palchik, A. Gedanken, J. Mater. Chem. 11 (2001) 869–873.
[15] Y.P. Fang, A.W. Xu, R.Q. Song, H.X. Zhang, L.P. You, J.C. Yu, H.Q. Liu, J. Am. Chem. Soc. 125 (2003) 16025–16034.
[16] K. Rajesh, P. Shajesh, O. Seidel, P. Mukundan, G.K. Warrier, Adv. Funct. Mater. 17 (2007) 1682–1690.
[17] W. Bu, L. Zhang, Z. Hua, H. Chen, J. Shi, Cryst. Growth Des. 7 (2007) 2305–2309.
[18] J. Lin, Y. Huang, J. Zhang, X. Ding, S. Qi, C. Tang, Mater. Lett. 61 (2007) 1596–1600.
[19] J. Lee, Q. Zhang, F. Saito, J. Alloys Compd. 348 (2003) 214–219.
[20] S. Wang, G. Zhou, M. Lu, Y. Zhou, S. Wang, Z. Yang, J. Am. Ceram. Soc. 89 (2006) 2956–2959.
[21] J. Sheng, S. Zhang, S. Lv, W. Sun, J. Mater. Sci. 42 (2007) 9565–9571.
[22] Y. Zhang, K. Han, T. Cheng, Z. Fang, Inorg. Chem. 46 (2007) 4713–4717.
[23] B. Tang, J. Ge, C. Wu, L. Zhuo, Z. Chen, Z. Shi, Y. Dong, Nanotechnology 15 (2004) 1273–1276.
[24] G. Guo, F. Gu, Z. Wang, H. Guo, J. Cryst. Growth 277 (2005) 631–635.
[25] X. Wang, M. Wang, H. Song, B. Ding, Mater. Lett. 60 (2006) 2261–2265.
[26] M.F. Vignolo, S. Duhalde, M. Bormioli, G. Quintana, Appl. Surf. Sci. 197 (2002) 522–526.
[27] K.S. Suslick, G.J. Price, Annu. Rev. Mater. Sci. 29 (1999) 295–326.
[28] F. Li, X. Liu, Q. Qin, J. Wu, Z. Li, X. Huang, Cryst. Res. Technol. 44 (2009) 1249–1254.
[29] S. Zhu, H. Zhou, M. Hibino, I. Honma, M. Ichihara, Adv. Funct. Mater. 15 (2005) 381–386.
[30] W. Lv, B. Liu, Q. Qiu, F. Wang, Z. Luo, P. Zhang, S. Wei, J. Alloys Compd. 479 (2009) 480–483.
[31] R. Jenkins, R.L. Snyder, Chemical Analysis: Introduction to X-ray Powder Diffractometry, John Wiley & Sons, Inc., New York, 1996, p. 90.
[32] X. Ma, H. Zhang, Y. Ji, J. Xu, D. Yang, Mater. Lett. 58 (2004) 1180–1182.
[33] M. Zhou, J. Yuan, W. Yuan, Y. Yin, X. Hong, Nanotechnology 18 (2007) 405704–405710.
[34] P. Pasierb, S. Komornicki, M. Rokita, M. Rekas, J. Mol. Struct. 596 (2001) 151–156.
[35] T.L. Van, M. Che, J.M. Tatibouet, M. Kermarec, J. Catal. 142 (1993) 18–26.
[36] S. Bernal, F.J. Botana, R. Garcia, J.M. Rodriguez-Izquierdo, React. Solids 4 (1987) 23–40.
[37] G. Adachi, N. Imanaka, Chem. Rev. 98 (1998) 1479–1514.
[38] S. Bernal, G. Blanco, J.J. Calvino, J. Solid State Chem. 180 (2007) 2154–2165.